minerals

MDPI

Article

Intercalation of Nontronite Clays from Santa Elena, Ecuador, Using Different Surfactant Hydrophobicity

Andres F. Rigail-Cedeño [1,2,*], Mauricio H. Cornejo [1,3,*], Julio A. Cáceres-Zambrano [3], Johanna S. Alava-Rosado [1] and Gladys García-Mejía [1,2]

[1] Faculty of Engineering in Mechanics and Production Sciences, ESPOL Polytechnic University, Campus Gustavo Galindo, Km 30.5 vía Perimetral, Guayaquil P.O. Box 09-01-5863, Ecuador
[2] Plastic Processing Laboratory, ESPOL Polytechnic University, Campus Gustavo Galindo, Km 30.5 vía Perimetral, Guayaquil P.O. Box 09-01-5863, Ecuador
[3] Center of Nanotechnology Research and Development (CIDNA), ESPOL Polytechnic University, Campus Gustavo Galindo, Km 30.5 vía Perimetral, Guayaquil P.O. Box 09-01-5863, Ecuador
* Correspondence: arigail@espol.edu.ec (A.F.R.-C.); mcornejo@espol.edu.ec (M.H.C.)

Abstract: The research of organoclays has been occurring for many years to develop and add value to these inorganic materials for several industrial applications, such as pollutant absorbers or impermeable plastics. The organoclay applications are intrinsically related to organo-modification and the structure of clays. This study shows the preparation and characterization of organoclays produced by a nontronite type clay (calcic bentonite) from the Tosagua Formation in the peninsula of Santa Elena in Ecuador. These clays were purified and centrifuged before organo-treatment. The purification and separation processes were used to remove organic matter and carbonates, and a cationic interchange from calcic to sodic (Ca^{2+} to Na^{+}) was carried out. Organo-modification was performed using two types of cationic compounds, i.e., Oleylmethylbis (2-hydroxyethyl) ammonium chloride and Di (hydrogenated tallow alkyl) quaternary amine to organoclay with different surface hydrophobicity. The samples were characterized by X-ray diffractometry (XRD), infrared spectrometry (FT-IR), thermo-gravimetry (TGA), and scanning electron microscopy (SEM) to analyze the effect after the mentioned treatment and the resulting organoclays by the addition of these surfactants. The results confirm the significant intercalation of the organic treatment suitable for environmental remediation, compatibilizing recycled plastics, or improving performance in different hydrophobicity systems for industrial applications.

Keywords: Tosagua Formation; organoclays; cationic surfactant; montmorillonite; nontronite

check for updates

Citation: Rigail-Cedeño, A.F.; Cornejo, M.H.; Cáceres-Zambrano, J.A.; Alava-Rosado, J.S.; García-Mejía, G. Intercalation of Nontronite Clays from Santa Elena, Ecuador, Using Different Surfactant Hydrophobicity. *Minerals* **2023**, *13*, 272. https://doi.org/10.3390/min13020272

Academic Editors: Jianxi Zhu and Janos Kristof

Received: 17 November 2022
Revised: 6 February 2023
Accepted: 9 February 2023
Published: 15 February 2023

Copyright: © 2023 by the authors. Licensee MDPI, Basel, Switzerland. This article is an open access article distributed under the terms and conditions of the Creative Commons Attribution (CC BY) license (https://creativecommons.org/licenses/by/4.0/).

1. Introduction

Organoclay is still one of the most used nanomaterials, presenting interesting morphological and chemical variations, thus being used in several industrial applications and environmental protection [1]. Remarkably, the market segmentation of organoclays is related to applications such as coatings, pesticides, oil-based drilling fluids, plastics, cosmetics, membranes, and lubricants [1]. The global market is currently about USD 971 million, which is expected to grow to 1.680 million by 2028 [2].

Such industrial applications are related to their intrinsic clay properties, such as high cation exchange capacity and organo-treatment. A significant area of the use of mineral clays is the absorption of heavy metals for removal from an aqueous solution. The advantages of using clays as an alternative sorbent are high ion absorption/exchange capacity, low permeability, mechanical and chemical stability, and large specific surface area [3]. The clays in Ecuador are mainly used in the construction industry or as a refractory material [4], so there is excellent potential for other added-value applications and the preparation of new materials [5].

New alternatives in clay modifications have led to new kinds of organoclays to tailor industrial applications. The evidence suggests that the intercalation due to cationic, anionic, or amphiphilic compounds has been extensively used to synthesize organoclays successfully [6,7]. Montmorillonite is widely available worldwide and is one of the most abundant and low-cost naturally occurring clay minerals [6]. For this reason, the hydrophobicity of organic montmorillonite by intercalating several surfactants is vital to optimize the interaction capacity used in polymer, geotechnical, or petroleum applications [8].

Clay-science literature suggests that the resulting organoclay's sorption characteristics are influenced principally by the properties of unmodified clay minerals and the properties of the intercalated organic matter [6]. The type of surfactant affects the structure of the modified clays, which means that interlayer distance can be tunable depending on the surfactant's chain length [9]. Likewise, clay chemistry and its cation exchange capacity (CEC) also play an essential role in forming intercalated structures. For instance, dialkylammonium cationic surfactants were successfully intercalated in silica layers, obtaining paraffinic structures at a broad range of CEC from 60 to 100 (meq/100 g) [10]. Sarkar et al. [10] revealed that basal spacing increases gradually with alkyl chain length. Despite its synthesis importance, the relationship between surfactant and clay chemistry is not well understood yet [11].

Morales A. et al. [12] studied the bentonites of the provinces of Santa Elena and Guayas, describing that these clays are of the "calcic bentonite" type, belonging to the group of dioctahedral smectites (ferruginous montmorillonites), with intercalations of illite and a slight presence of chlorite-kaolin. The origin comes mainly from the alteration of Andean volcanic ash deposited on the sea bottom where climatic conditions do not affect their chemistry. Some studies have previously characterized calcic nontronite-type clay belonging to the Tosagua Formation of the Dos Bocas member of the Santa Elena Peninsula, Ecuador [12,13]. These studies have focused on developing polymer nanocomposites with organoclays produced from the Ancon Formation of the Santa Elena peninsula.

The bentonites used for this study are in the west part of Ecuador, specifically in the province of Santa Elena (Via a la Costa), along with the towns of Buenos Aires and Sucre (Latitude: 80–81°, Longitude: 2–3°) as shown in Figure 1. These clays are located within the Progreso Basin and correspond to geological formations of ages from the upper Oligocene to the middle Miocene. The basal part in the sector is the Zapotal member, which outcrops at the basin's edges, consisting of coarse-grained sandstone tuffs and chert conglomerates; it is a formation with high silica content. The upper part is the Dos Bocas Formation, with thicknesses between 300 and 2360 m. It comprises several layers of silty claystone and dark brown siltstones (studied clays) with carbonates (calcareous concretions). These siltstone layers are intercalated with lignite and gypsum veins with iron and manganese oxides. However, these claystone layers have silty levels and sandstones with high quartz contents. In addition, possessing thicknesses between 300 and 600 m, the Villingota Formation is found nearby and is composed of thin layers of silty claystone and gray or white diatomaceous earth [12,13].

A geological profile was carried out within the Villingota mining concession. The sample used for this study is a composite obtained from the crushing plant of the concession. The geological characteristics mentioned above are observed in particular layers of greenish clays and levels with sedimentary sulfur as is shown in Figure 2.

This research aims to study the development of organoclays from natural nontronite clays from the coastal region of Ecuador. Most literature has studied montmorillonite clay types to develop organoclays. The organoclays must be characterized by experimental techniques, such as XRD, FTIR, SEM, and TGA-DSC. Developing such organoclays and their resultant structure deserves special attention and has been discussed.

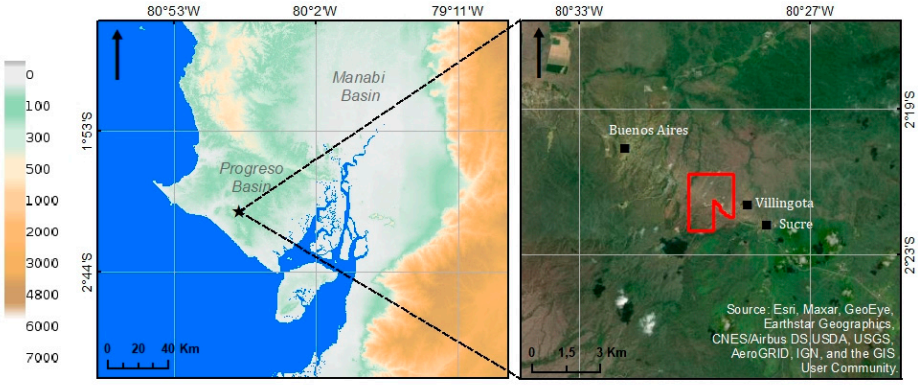


Figure 1. Location map of the study area in Santa Elena Province, Ecuador. Universal Transverse Mercator Projection (WGS 84—17S). Elevation data and satellite image information from Instituto Geográfico Militar (http://www.geoportaligm.gob.ec/dtm/wms (accessed on 28 February 2022), Esri, Maxar, Geoeye, Earthstar geographics, CNES/Airbus DS, USDA, USGS, AeroGRID, IGN, and the GIS User Community.

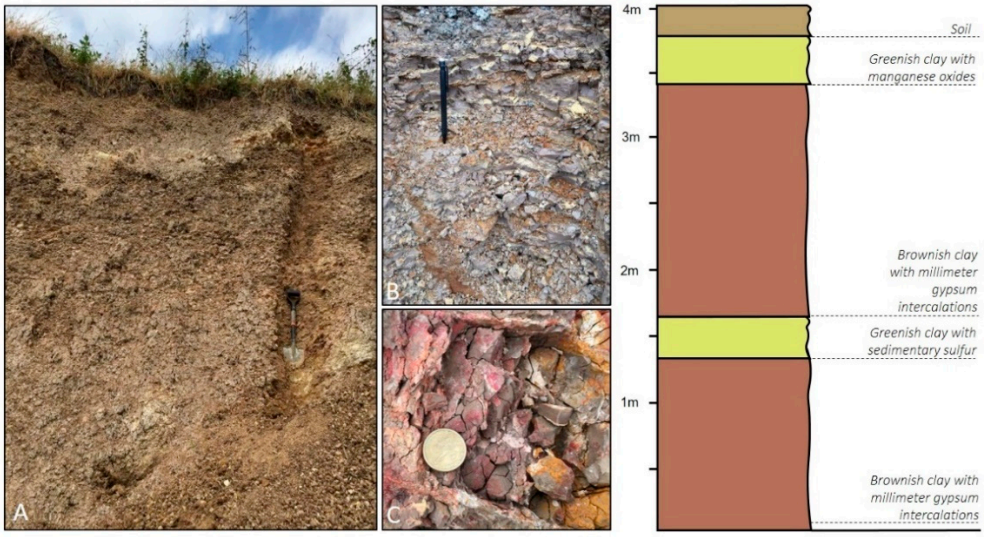


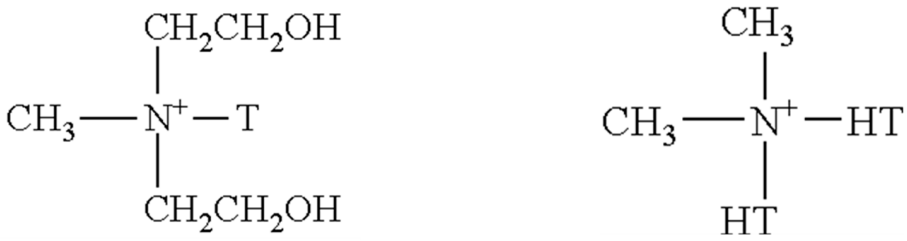
Figure 2. Outcrop (**A**–**C**) and geological column of the natural clays, iron, and manganese oxides that can be observed in some areas of the study area, the Dos Bocas formation, Santa Elena province, Ecuador.

Although there is a large amount of data on the use of surfactants for the modification of clays in previous literature, in this context, the benefits of the purification procedure followed to obtain the Ecuadorian organoclays and their characterization allow for determining a range of industrial applications. The findings of this research are expected to offer remarkable possibilities for advancing the development of local organoclays to meet the needs of regional industries in the years to come.

2. Materials and Methods

Calcic, naturally occurring smectite-type clay, Nontronite Ca^{2+}, from the Tosagua Group, Santa Elena, Ecuador, was used as a raw material in this study [12]. As the first step in organoclay development, purification treatment and cationic exchange were carried out to obtain a sodic smectite clay, Nontronite Na^{+}, which was used to mix them with alkylammonium salts to obtain organoclays.

The surfactants used to obtain organoclays were purchased from AkzoNobel, Fort Worth, USA. The chemical structures of the surfactants used to modify the sodic nontronite are shown in Figure 3.



(**a**) (**b**)

Figure 3. Chemical structures of (**a**) Oleylmethylbis (2-hydroxyethyl) ammonium chloride and (**b**) Di (hydrogenated tallow alkyl) quaternary amine.

The quaternary ammonium salts were used to prepare the organoclays a) NFT1: Oleylmethylbis (2-hydroxyethyl) ammonium chloride (commercial surfactant name: ETHOQUAD O/12 PG) and b) NFT2: Di (hydrogenated tallow alkyl) quaternary amine (commercial surfactant name: ARQUAD 2HT-75). The resulting organoclays are given in Table 1.

Table 1. Description of organoclay compounds.

Sample	Formulation
Nontronite Ca^{2+}	Natural clay (untreated)
Nontronite Na^{+}	Purified natural clay with cationic exchange
NFT1	Nontronite Na^{+} + Oleylmethyl [ethoxylated (2)]
NFT2	Nontronite Na^{+} + Di (hydrogenated tallow alkyl)

2.1. Organoclay Preparation

The smectite content can be improved by removing the gangue compounds associated with weathering or the composition of the rock, such as humic acids (organic components), iron oxides, carbonates, quartz, and feldspars, among others. Quartz and clays, such as kaolinite, can be removed by granulometric methods if their particle size is more significant than smectites (≥2 μm), such as by sieving, magnetic separation, and gravimetric separation (particle settling speed—Stokes Law). Previously, a reduction in grain size and separation was performed through ultrasound and centrifugation treatments [14]. Figure 4 shows the scheme of the previous purification process to prepare the organoclay.

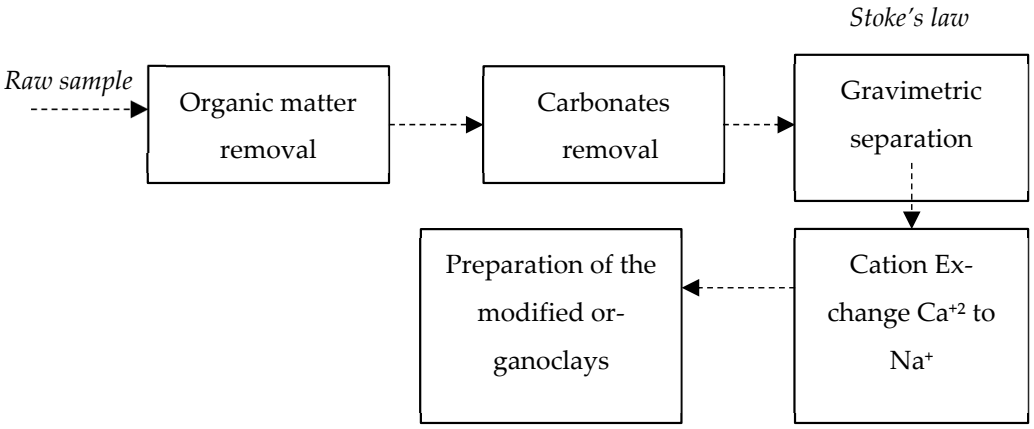


Figure 4. Organoclay preparation scheme.

2.1.1. Organic Matter Removal

Initially, the clay aggregates were ground using a Retsch PM 100 ball mill. An amount of 50 g of clay was dispersed in 50 mL of distilled water using beakers, as shown in Figure 5a. To remove the organic matter, successive doses of 10 mL of hydrogen peroxide (10%) were added and stirred with a glass rod until the reaction with the organic matter was stopped (about 50 mL was used). The solution was left to stand for at least 12 h in an oven at 60 °C. An additional 10 mL of hydrogen peroxide was added to verify no further reaction. The solid phase was separated by centrifugation at 3000 rpm for 5 min. In this process, 50 mL of distilled water was added to the separated bentonite and stirred with the glass rod, and the solution was allowed to settle down; then, the excess water was removed, and the procedure was repeated three times. Finally, it was dried for 24 h at 60 °C in the oven.



(**a**) (**b**)

Figure 5. Calcium nontronite purification treatment. (**a**) Removal of organic matter, (**b**) gravimetric separation (Stokes' Law).

2.1.2. Carbonate Removal

After the organic matter removal, the sample was ground in an agate mortar, and 60 mL of distilled water was added to the sample. Three successive doses of 10 mL of hydrochloric acid (10%) were added and stirred with a glass rod until the reaction with the carbonates was stopped, as is shown in Figure 5b. An additional 10 mL of hydrochloric acid (10%) was added to verify no reaction. When the reaction with the carbonates stopped, the same procedure of solid phase separation mentioned in the purification phase was repeated.

2.1.3. Gravimetric Separation

To obtain the clay fraction and eliminate the more significant amount of gangue minerals, gravimetric separation (Stokes' Law) was used. A 20 g sample was taken and mixed with 100 mL of distilled water, adding 10 mL of 1N concentration sodium hydroxide; allowed to settle overnight; and then stirred with a homogenizer (mechanical shaker) at 120 rpm for 30 min. It was then sieved through an ASTM #400 mesh (38 μm) and then placed in a 1000 mL beaker, completing the volume with distilled water, and stirred for 20 s.

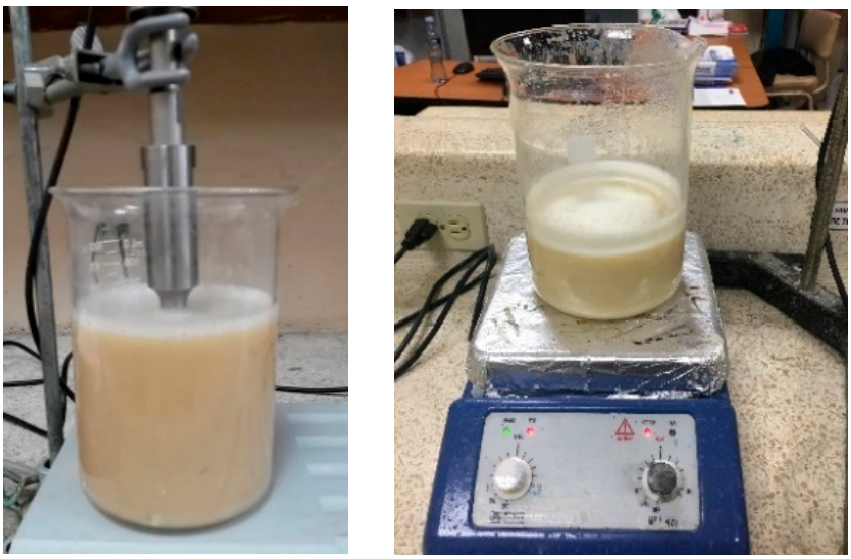
2.1.4. Cation Exchange Process

To obtain Nontronite Na^+, the calcium cation was replaced by the sodium cation obtained from sodium chloride. A 60 g sample from the previous step was placed in a 1 M sodium chloride solution, mixed, and placed in the centrifuge for 5 min at 3500 rpm. The supernatant liquid was removed, and the sample was washed several times with distilled water until it did not settle easily, and it was then dried at 60 °C. Nontronite Na^+ (42 g) was

mixed in one liter of distilled water, then passed through a separatory funnel and left to settle for 24 h. The purge was opened, and the swollen part of the sample was collected and dried at 60 °C.

2.1.5. Preparation of the Modified Organoclays

An amount of 7.5 g of Nontronite Na^+ was mixed in a 600 mL water/ethanol (4:1) solution [15] in a magnetic stirrer at 300 rpm for 2 h with a temperature of 60 °C. Alkylammonium salt (10 g) in 200 mL of distilled water was added and mixed with an ultrasonic processor as is shown in Figure 6a. Thus, the loading of the surfactant compounds was 2:1 surfactant-clay (*w*/*w*). The ultrasonic conditions for the mixture are at 50% amplitude for 1 h and subsequently with a magnetic stirrer at 300 rpm for 5 h at 60 °C as is shown in Figure 6b. A water/ethanol (1:1) solution was added, centrifuged at 3500 rpm for 5 min, and excess liquid removed. The solution was dried at 60 °C, ground in an agate pestle, and sieved to 45 μm.



(**a**) (**b**)

Figure 6. Preparation of nanoclay in ultrasonic processor (**a**) and magnetic stirrer (**b**).

2.1.6. Determination of Cation Exchange Capacity (CEC)

The CEC was determined by the methylene blue (MB) method according to ASTM D 5890-95 [16]. The CEC was calculated using Equation (1):

$$CEC = \frac{V.N}{m} \times 100 \quad (1)$$

where *CEC* is the cation exchange capacity (meq/100 g), *V* is the volume of methylene blue used in the process (mL), *N* is the milliequivalent value of 1 mL of methylene blue, and *m* is the content of clay used (g).

2.2. Characterization

2.2.1. Quantitative X-ray Diffractometry (QXRD)

Mineralogical composition and increased basal spacings of the clays were obtained using a Panalytical X'Pert-Pro diffractometer with a conventional X-ray tube (CuKα radiation) and a multichannel X'Celerator detector. The operating conditions were 45 kV and 40 mA, with 0.05° step, 20 s scanning time per step, with 1/4 mm aperture at the incident and 10 mm mask, between angles 5° and 70° (2θ).

A Rietveld refinement for quantitative analysis was carried out in the samples before and after the purification treatment; for this, 1 g of sample was used, comprising 90% *w*/*w* clay and 10% *w*/*w* ZnO, an internal standard that allows the quantitative analysis of the samples. Then these were homogenized and placed inside the sample holders of the equipment. The diffractograms were quantified with the X'pert HighScore Plus software, Version 2.2.3 from Malvern Panalytical Ltd., Malvern, UK.

The refinement consisted of adjusting the global parameters, such as baseline, sample offset, and lattice parameters, and then adjusting them to the parameters of the profiles. The adjustments were refined using the 15-parameter "Chebyshev II" function. After several refinement attempts, the following indices were obtained: weighted R percent (Rwp) of 4.47 and goodness of fit (GOF) of 9.07.

A qualitative analysis was also carried out to verify the intercalation of alkylammonium salts in the treated clay (Nontronite Na^+) in NFT1 and NFT2 samples, with the same operating conditions mentioned.

2.2.2. Fourier Transform Infrared Spectrometry (FTIR)

A Perkin Elmer Spectrum 100 FTIR transmittance spectrometer was used between 400 and 4000 cm^{-1}, with a resolution of 4 cm^{-1}. For the tests to run, samples were diluted in KBr (1 mg of sample per 150 mg of KBr), homogenized, and subjected to a pressure of 15 t/m^2, thus obtaining a pellet. The graphs were processed using SpectraGryph spectroscopy software from Optical Spectroscopy Software, Oberstdorf, Germany.

2.2.3. Thermo-Gravimetric Analysis (TGA)

The weight loss and degradation were analyzed using a thermo-gravimetric analyzer (TA instruments Q600 SDT). The TGA curves were processed using TA Universal Analysis 2000 software from TA instruments, New Castle, USA. A sample of 10 mg was placed in an alumina crucible, and the temperature was raised from 25 to 600 °C, at a rate of 10 °C/min, in a high-purity nitrogen atmosphere.

2.2.4. Scanning Electron Microscope (SEM)

The morphology of the samples was obtained using an FEI Inspect S50 scanning electron microscope, operating at 7.5 kV in high vacuum with a pressure of 35–40 Pa. In addition, a sputter-coater was used for the gold–palladium coating (EMITEC brand, model SC7620), with a pressure of 5 mbar, a current of 18 mA, and an argon atmosphere, to improve the electrical conductivity of these ceramics.

3. Results and Discussion

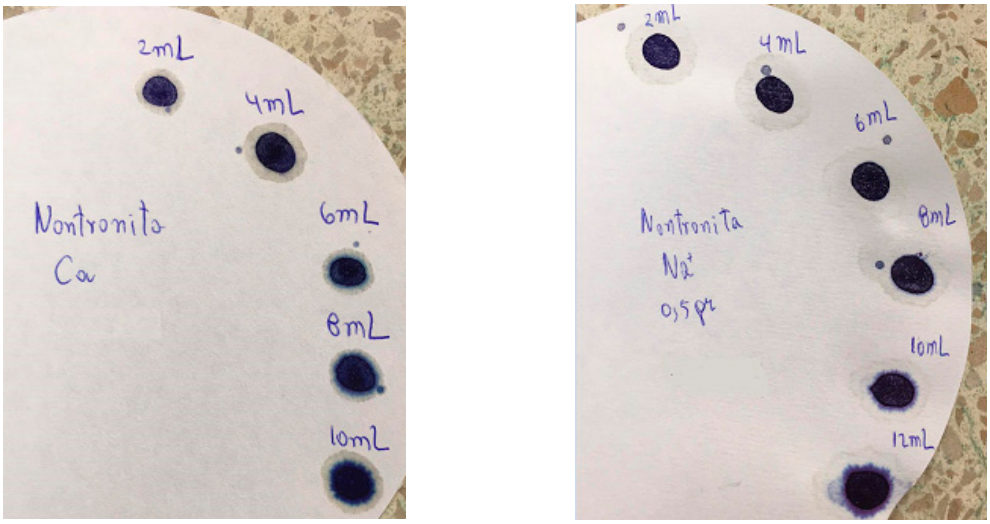
3.1. Cation Exchange Capacity

The organic cation exchange at the silicate surface is a function of the base clay's cation exchange capacity (CEC) as is shown in Figure 7a,b. The CEC is defined as the number of cations (meq/100 g) that can be substituted with other cations to the mass of clay and is a measure of the degree of isomorphic substitution that can occur in silicate layers [14].

Table 2 shows the cation exchange capacity of the clays before and after the purification treatment using the same procedure described in Section 2.1. The increased cation exchange capacity of the natural clay can be noticed after the purification treatment.

3.2. X-ray Diffractometry (XRD)

X-ray diffraction allowed recognition of the minerals contained in the total fraction of the samples before and after the purification treatment. The treatment increased the content of clays. In this case, the content of Nontronite Na^+ increased to 53.7% after the purification process, as seen in Table 3, and decreased by ~60% in quartz, ~25% in feldspar, and 100% in illite content.



(**a**) (**b**)

Figure 7. Cation exchange capacity testing. (**a**). Nontronite Ca^{2+}. (**b**). Nontronite Na^{+}.

Table 2. Details of the cation exchange capacity of the clays.

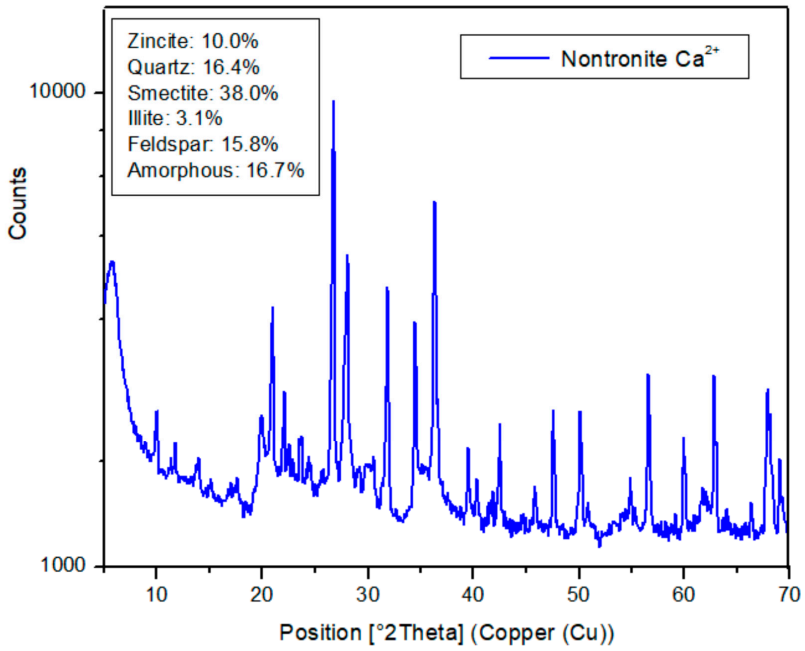
Sample	CEC (meq/100 g)
Nontronite Ca^{2+}	56
Nontronite Na^{+}	67

Table 3. Content of calcium and sodium nontronite obtained by XRD (%wt).

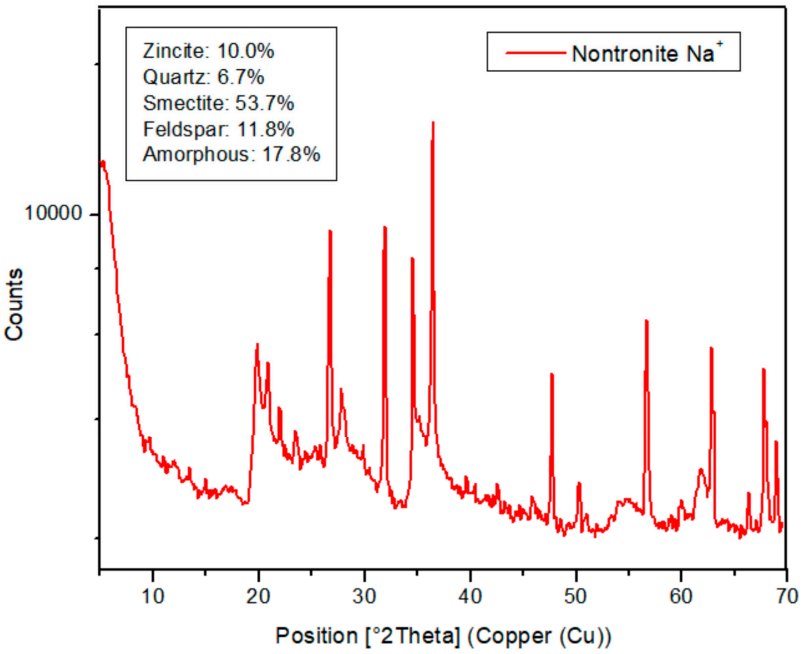
Sample	Quartz	Feldspars	Smectite	Illite	Amorphous
Nontronite Ca^{2+}	16.4	15.8	38	3.1	16.7
Nontronite Na^{+}	6.7	11.8	53.7	0	17.8

Figure 8a,b show the characteristic peak of sodium clays, which is in the range of 6–8°, with an approximate interplanar distance (d001) of 12.4 Å; generally, the basal space of calcic smectite is around ~15 Å [13]. This difference in basal spacing is due to the size of the atomic radius of sodium, which is smaller than calcium; this explains why sodium clays have a greater swelling capacity. For this reason, the cationic exchange from Ca^{2+} to Na^{+} was carried out so that our sodium clay can absorb more surfactant between its layers and thus facilitate a better intercalation.

Figure 9 shows that the characteristic peak of the first diffraction observed in the treated clay is shifted to an offset angle of ~2–3° for both organo-modified clays (NFT1 and NFT2). This phenomenon represents an exchange cation with the alkylammonium salt due to the higher basal (~37.9 Å) spacing than Nontronite Na^{+} (~12.4 Å). An increase in basal spacing is referred to as good intercalation of the cationic compounds in the clay layers. The basal spacing seems to be related to large hydrophobic groups on surfactants and the decrease in surface energy [10]. Similarly, this effect is also observed in the NFT2 diffractogram, where the organo-nontronite presents the highest peak at 38.1 Å. These basal spacings are related to a pseudo-molecular orientation of the alkylammonium ions into the silicate layer [7]. Both arrangements are consistent to the long chain of the surfactant and the high surfactant loading used in this research. Surfactants were observed due to the basal spacings in both organoclays NFT1 and NFT2 [17].



(**a**)



(**b**)

Figure 8. Diffractograms (**a**). Natural clay (Nontronite Ca^{2+}) (**b**). Clay with purification treatment (Nontronite Na^{+}).

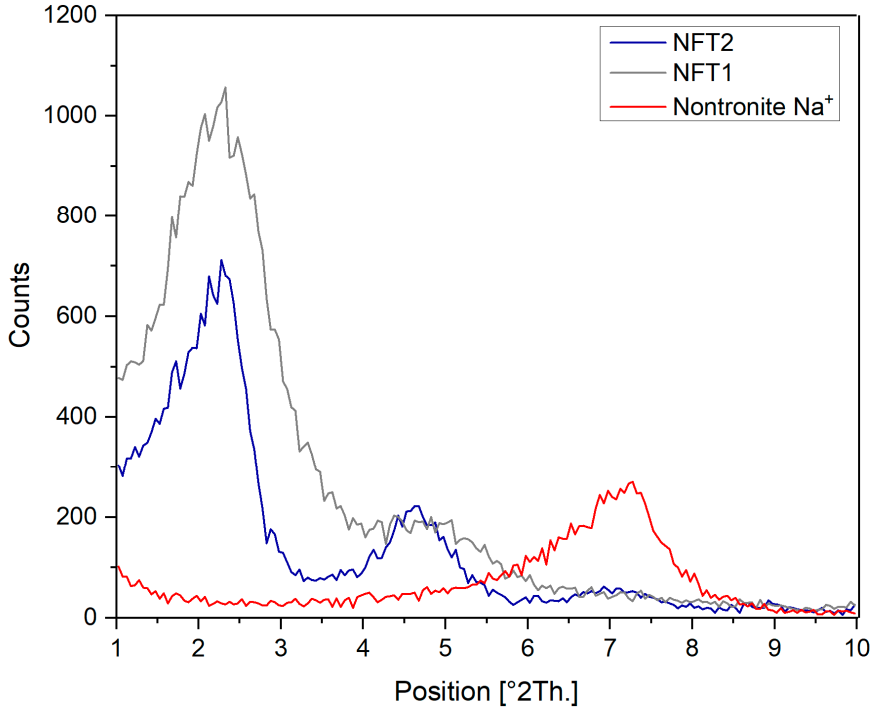


Figure 9. Diffractograms of Nontronite Na^+ and organoclays NFT1 and NFT2.

3.3. Fourier Transform Infrared Spectrometry (FTIR)

Figure 10 shows the prominent FTIR peaks for all clays with and without treatments [18,19]. Nontronite clays present the following functional groups, such as bands around ~3626 cm^{-1} and ~3440 cm^{-1} corresponding to the stretching vibrations of Fe(OH)Fe bonds; this double band suggests that Fe is found in two slightly different environments in the octahedral sheet [19–21] and vibration bands due to the stretching of the OH groups at 3440 cm^{-1} [19,21]. Vibrations of SiO stretching and Si-O-Al bending bands occur at ~1027 cm^{-1} and ~526 cm^{-1} correspondingly, while Al_2OH and AlMgOH bending bands are observed at ~918 cm^{-1} and ~874 cm^{-1}, respectively [20]. Nevertheless, a band for the fingerprint around ~698 cm^{-1} corresponds to FeO in nontronites with higher iron content [21].

Additionally, the appearance of new vibrational bands is evident due to the addition of surfactants. The bands around ~2922 cm^{-1} and ~2852 cm^{-1} correspond to the asymmetric and symmetric stretching vibrations of the CH_2 bands, respectively [18,22], as shown in Figure 10 and Table 4. The vibrations produced by the scissoring bend belonging to the CH_2 bands are observed at ~1467 cm^{-1}. The characteristic bands of the organoclays NFT1 and NFT2 are still maintained after modification by the surfactants, as shown below.

Table 4 and the plot evidence that there is a shift towards lower wavenumbers of the bands corresponding to the vibration by the CH_2 scissoring bending at ~1470 cm^{-1}, belonging to the surfactants [23]. This wavenumber shift phenomenon is due to the sensitivity of interchain interactions and the chain packing arrangement of the surfactant that is intercalated between the layers of the clays [24], which in turn causes an increase in the interplanar distance of the NFT1 organoclays due to the structure of the surfactant used. A similar phenomenon to the previous one is observed in the NFT2 organoclay. The values of the asymmetric stretching vibration CH_2 probe the nature of the paraffin/type structure in both organoclays. Disordered structure promotes a dense packing of the chain in the silicate layers [24].

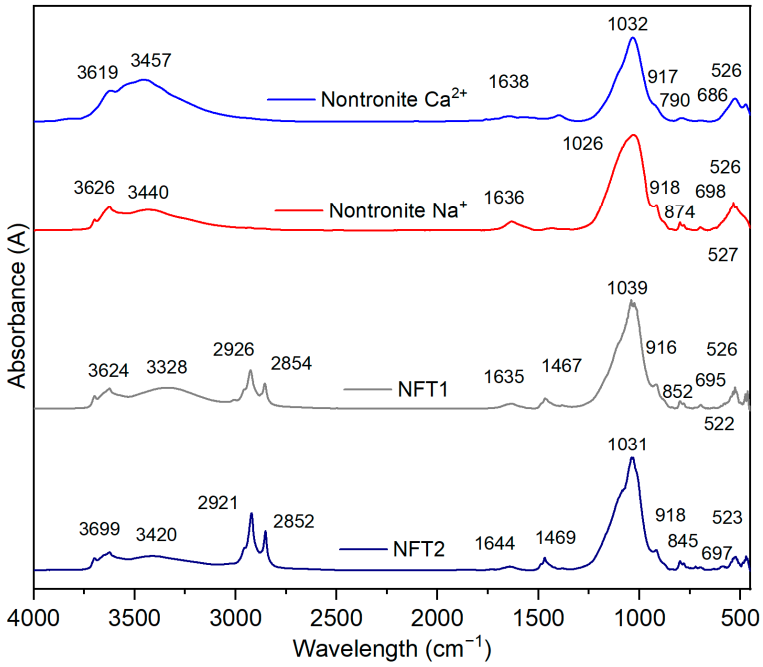


Figure 10. FTIR of treated and non-treated clays.

Table 4. Position (cm^{-1}) and assignments of the prominent bands of the modified and unmodified clays [25,26].

Nontronite Ca^{2+}	Nontronite Na^{+}	NFT1	NFT2	Assignment
3619	3623	3624	3699	Stretching vibrations of Fe(OH)Fe bonds
3457	3440	3328	3420	Stretching vibrations of Fe(OH)Fe bonds
1638	1637	2926	2921	Asymmetric stretching vibration of CH_2 bands
-	-	2854	2852	Symmetric stretching vibration of CH_2 bands
-	-	1635	1644	Bending vibration of the OH bonds
-	-	1467	1469	Scissoring bending vibrations of the CH_2 bands
1032	1027	1039	1031	Stretch vibrations of the SiO
917	918	916	918	Flexural vibration of the Al_2OH bands
790	874	852	845	Flexural vibration of the AlMgOH strips
686	698	695	697	Vibrations of the bands corresponding to the FeO group
526	526	526	523	Bending vibrations of the Si-O-Al strips

3.4. Thermo-Gravimetric Analysis (TGA)

Figure 11 shows the treated clay and organoclay thermo-gravimetric analysis and reveals the different temperature zones where mass loss is evident. The TGA of the treated clay from Tosagua has three loss steps between ambient and 100 °C, at ~250 °C and ~470 °C [10,27]. The mass loss steps are related in the first phase to the desorption of water from the clay, dehydration of the Na^{+} cation in the interlayer, and finally, the dihydroxylation of the Nontronite. The peaks at around 450 and 600 °C represent the endothermic peaks of dehydroxylation as is evidenced in Figure 12; all these are characteristic of the smectite series [13]. The mass loss percentage decreases considerably after the addition of the surfactant (NFT1 and NFT2) during the first phase of degradation below 250 °C due to the loss of water molecules.

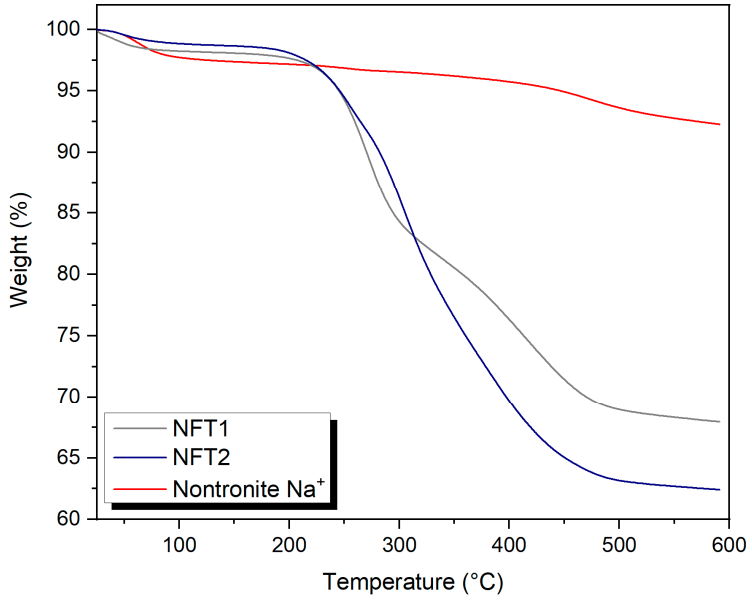


Figure 11. Thermal decomposition of treated clay and organoclays.

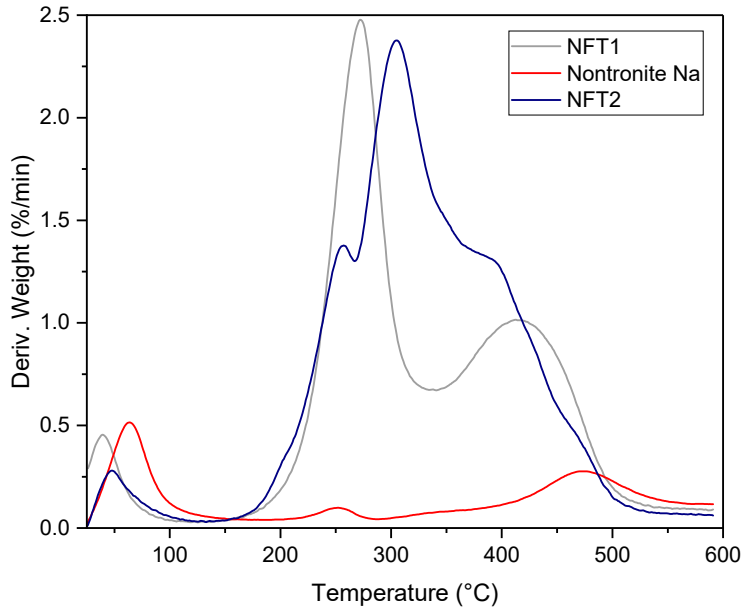


Figure 12. DTG plot of treated clay and organoclays.

The differential TG plot (Figure 12) shows again that the intervals of decomposition of intercalated surfactant in the organoclay take place in three stages where there are considerable mass losses due to: (a) surfactant cations intercalated in the intermediate layers of the clays, caused by the cation exchange performed, and attached to surface sites by electrostatic interaction; (b) surfactant (cations and molecules) physically adsorbed on the external surface of the clay; and (c) molecules of the surfactants located within the intermediate layer of the clay [28]. The initial decomposition of NFT1 occurs around 40 °C (T1), and there is a mass loss corresponding to the water molecules located on the surface of the organoclay. Surfactant degradation (stages b and c) occurs at around the following temperatures: 270 °C (T2) and 420 °C (T3), respectively. Additionally, two phenomena that occur at the time of performing these thermal tests can be observed: (a) there is more significant degradation of the surfactant, and (b) there is a slight improvement in the intercalation of the surfactant in the organoclay processed with Ecuadorian raw material (NFT1) at ~421 °C (T3). In addition, the hydrophobicity of the NFT1 caused by the use of

the surfactant can be evidenced since the same degradations caused by the water vapor do not appear in comparison to the nontronite Na+. The decomposition of NFT1 has its highest weight loss around 270 °C and 420 °C due to the degradation of the surfactant [28]. The decomposition NFT2 shows more stages of degradation mentioned above regarding the consumption of the surfactant. The decomposition of NFT2 has its highest weight loss around 300 °C and 400 °C due to surfactant degradation.

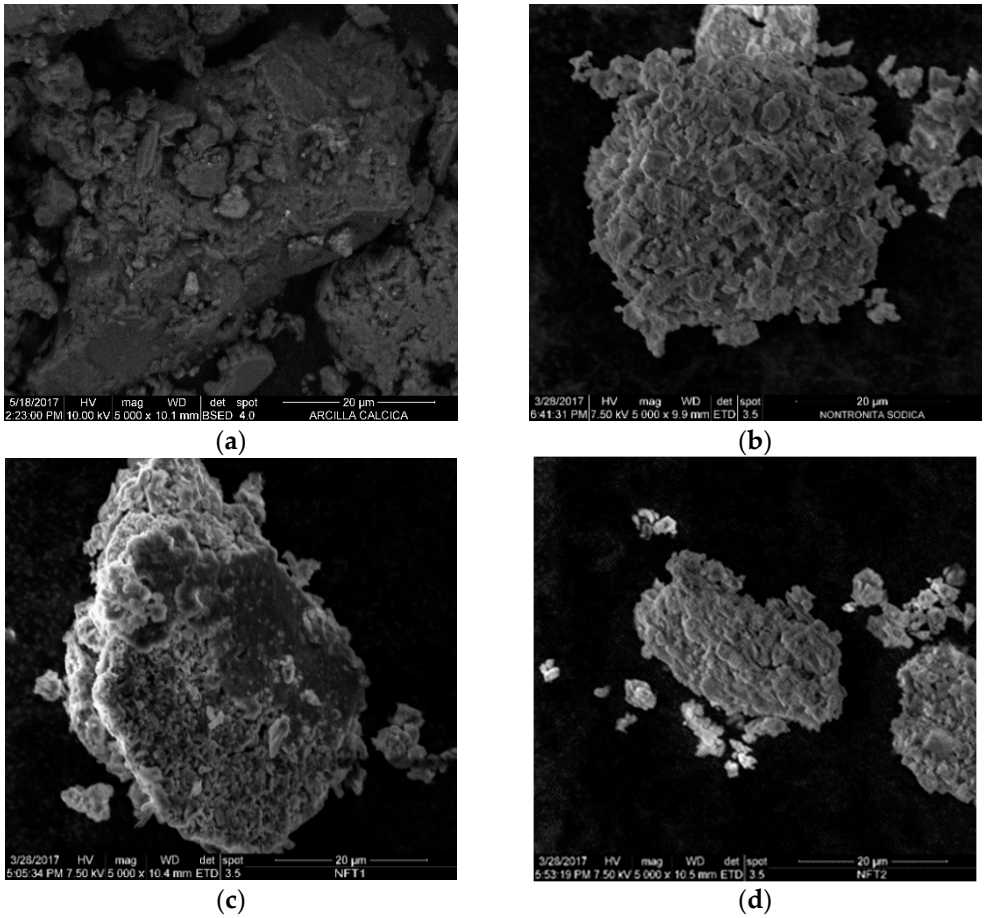
Additionally, results show that the thermal properties are enhanced in NFT1 compared to NFT2. Table 5 shows the degradation temperatures of the organoclays, where the excess of the surfactant used can be seen because the percentage of degradation increases in the temperature range where the alkylammonium salt used is degraded.

Table 5. Degradation temperatures and mass loss of clays and organoclays.

Sample	Mass Loss (%)	T1 (°C)	Mass Loss (%)	T2 (°C)	Mass Loss (%)	T3 (°C)	Mass Loss (%)	T4 (°C)
Nontronite Na^+	1.14	64	3.14	252	5.60	474	–	–
NFT1	0.65	41	10.49	272	26.17	421	–	–
NFT2	0.37	49	63.8	256	14.88	304	29.74	393

3.5. Scanning Electron Microscope (SEM)

Figure 13a,b show the surface morphology of natural and modified clay. The Nontronite Ca^{2+} presents a surface morphology typical of smectites, i.e., in intercalated layers or lamellae, while the Nontronite Na^+, after treatment, appears less intercalated and more agglomerated.



(**a**) (**b**) (**c**) (**d**)

Figure 13. SEM micrographs of (**a**) calcic and (**b**) sodic nontronite, (**c**) NFT1, and (**d**) NFT2 (5000×).

Figure 13c,d show the resulting organoclays. The micrographs show that both had similar behavior as the clay after purification and cation exchange treatment. NFT1 and NFT2 appear with regular faces, high-porosity structures, and some agglomerates. It indicates that the synthesis did not change the morphology of the treated clay.

4. Conclusions

This study contributes to the development of a new family of organoclays based on nontronite clay type. The characterization analyses through X-ray diffractometry identified nontronite-type clay as the principal mineral in the Tosagua formation (Dos Bocas). The economic impact is enormous for using natural nontronite as a raw material to obtain new organoclays for expanding several related industries.

The preparation and purification processes to obtain the Nontronite Na^+ show the procedure's effectiveness, since organic and inorganic matter were removed from Nontronite Ca^{2+} in the characterization analysis.

When the clays were modified as organoclays, they showed good intercalation of both surfactants in the nontronite layers. X-ray diffractometry indicated that the basal spacing of NFT1 (d_{001} = 37.7 Å) and NFT2 (d_{001} = 38.1 Å) suggests both surfactants' intercalation. These relatively high basal spacings indicate that these organoclays can be used in several organoclay applications. The results were supported by TGA, FTIR, and SEM results. TGA results show a decrease in the amount of free water in the organoclays and increasing degradation temperatures, confirming the intercalation of surfactants in the nontronite clays. The methylene and methyl groups from alkylammonium were observed by FTIR. The micrographs showed significant similarity concerning surface morphology between the diverse types of organoclays.

5. Future Work

Studies should perform additional treatments to improve the nontronite–quartz ratio and remove iron, thus obtaining clay with a higher degree of purity. To yield more sustainable materials, volatile organic compounds and bio-surfactants should be used to organophilize the clays for compatibilization of immiscible recycling plastics or developing biopolymer clay nanocomposites. The purification process and its resulting purity should be analyzed more deeply. Based on these results, the Ecuadorian organoclays obtained from Santa Elena, Ecuador, should be analyzed to obtain the feasibility of applications such as pollutant adsorption or polymer clay nanocomposites.

Author Contributions: Conceptualization, A.F.R.-C. and M.H.C.; methodology, A.F.R.-C.; software, J.A.C.-Z.; validation, A.F.R.-C., M.H.C. and J.A.C.-Z.; formal analysis, A.F.R.-C.; investigation, J.S.A.-R., G.G.-M. and J.A.C.-Z.; resources, A.F.R.-C., M.H.C. and G.G.-M.; data curation, J.A.C.-Z., G.G.-M. and J.S.A.-R.; writing—original draft preparation, J.S.A.-R. and A.F.R.-C.; writing—review and editing, G.G.-M. and A.F.R.-C.; visualization, G.G.-M.; supervision, A.F.R.-C.; project administration, A.F.R.-C. All authors have read and agreed to the published version of the manuscript.

Funding: This research received no external funding.

Data Availability Statement: The data presented in this study are available on request from the corresponding author.

Acknowledgments: The authors would like to thank the Centre of Investigation and Nanotechnology (CIDNA) and Materials laboratory (LEMAT) for their laboratory equipment support.

Conflicts of Interest: The authors declare no conflict of interest. The funders had no role in the design of the study; in the collection, analyses, or interpretation of data; in the writing of the manuscript; or in the decision to publish the results.

References

1. Singh, N.B. Clays and Clay Minerals in the Construction Industry. *Minerals* **2022**, *12*, 301. [CrossRef]
2. Global Organoclay Market Research Report 2022. Available online: https://www.industryresearch.co/global-organoclay-market-20779636) (accessed on 12 October 2022).

3. Awasthi, A.; Jadhao, P.; Kumari, K. Clay nano-adsorbent: Structures, applications and mechanism for water treatment. *SN Appl. Sci.* **2019**, *1*, 1076. [CrossRef]
4. Garzón, E.; Pérez-Villarejo, L.; Eliche-Quesada, D.; Martínez-Martínez, S.; Sánchez-Soto, P.J. Vitrification rate and estimation of the optimum firing conditions of ceramic materials from raw clays: A Review. *Ceram. Int.* **2022**, *48*, 15889–15898. [CrossRef]
5. Jaramillo-Fierro, X.; González, S.; Jaramillo, H.; Medina, F. Synthesis of the zntio3 /tio2 nanocomposite supported in ecuadorian clays for the adsorption and photocatalytic removal of methylene blue dye. *Nanomaterials* **2020**, *10*, 1891. [CrossRef] [PubMed]
6. Perelomov, L.; Mandzhieva, S.; Minkina, T.; Atroshchenko, Y.; Perelomova, I.; Bauer, T.; Pinsky, D.; Barakhov, A. The synthesis of organoclays based on clay minerals with different structural expansion capacities. *Minerals* **2021**, *11*, 707. [CrossRef]
7. de Paiva, L.B.; Morales, A.; Díaz, F.R.V. Organoclays: Properties, preparation and applications. *Appl. Clay Sci.* **2008**, *42*, 8–24. [CrossRef]
8. Santos, E.P.; Fook, M.; Malta, O.; de Lima, S.; Leite, I.F. Role of surfactants in the properties of poly(ethylene terephthalate)/purified clay nanocomposites. *Materials* **2018**, *11*, 1397. [CrossRef]
9. Gamoudi, S.; Frini-Srasra, N.; Srasra, E. Influence of synthesis method in preparation of HDTMA ± and HDPy ± illites/smectites. *Appl. Clay Sci.* **2015**, *116–117*, 78–84. [CrossRef]
10. Sarkar, M.; Dana, K. Intercalation of montmorillonite with dialkylammonium cationic surfactants. *J. Mol. Struct.* **2022**, *1256*, 132468. [CrossRef]
11. He, H.; Ma, L.; Zhu, J.; Frost, R.; Theng, B.; Bergaya, F. Synthesis of organoclays: A critical review and some unresolved issues. *Appl. Clay Sci.* **2014**, *100*, 22–28. [CrossRef]
12. Morales Carrera, A.M.; Varajão, A.F.D.C.; Gonçalves, M.A. Mineralogical charaterization of the clays of the Santa Elena Peninsula, Ecuador. *Rev. Esc. Minas* **2008**, *61*, 97–105. [CrossRef]
13. Morales-Carrera, A.M.; Varajão, A.; César-Mendes, J.; Carrión, P.C.M. Estado del arte de la arcilla de la provincia del Guayas y su proyección a la península de Santa Elena, Ecuador. *Bol. Geol. Min.* **2006**, *117*, 723–736.
14. Bahranowski, K.; Serwicka, E.M. Textural effects in powdered montmorillonite induced by freeze-drying and ultrasound pretreatment. *Appl. Clay Sci.* **2006**, *32*, 64–72. [CrossRef]
15. Lee, J.Y.; Lee, H.K. Characterization of organobentonite used for polymer nanocomposites. *Mater. Chem. Phys.* **2004**, *85*, 410–415. [CrossRef]
16. Çiftçi, H.; Ersoy, B.; Evcin, A. Synthesis, characterization and Cr(VI) adsorption properties of modified magnetite nanoparticles. *Acta Phys. Pol. A* **2017**, *132*, 564–569. [CrossRef]
17. Taleb, K.; Pillin, I.; Grohens, Y.; Saidi-Besbes, S. Gemini surfactant modified clays: Effect of surfactant loading and spacer length. *Appl. Clay Sci.* **2018**, *161*, 48–56. [CrossRef]
18. Slaný, M.; Jankovič, Ľ.; Madejová, J. Structural characterization of organo-montmorillonites prepared from a series of primary alkylamines salts: Mid-IR and near-IR study. *Appl. Clay Sci.* **2019**, *176*, 11–20. [CrossRef]
19. Franco, F.; Pozo, M.; Cecilia, J.; Benítez-Guerrero, M.; Lorente, M. Effectiveness of microwave assisted acid treatment on dioctahedral and trioctahedral smectites. The influence of octahedral composition. *Appl. Clay Sci.* **2016**, *120*, 70–80. [CrossRef]
20. Sklute, E.C.; Michalski, J.R. Structural and spectroscopic changes to natural nontronite induced by experimental impacts between 10 and 40 GPa. *J. Geophys. Res. Planets* **2015**, *120*, 888–912. [CrossRef]
21. Christidis, G.E.; Skarpelis, N. Clay Mineralogy Of The Sedimentary Iron-Nickel Ore Of Agios Ioannis, Ne Boeotia: New Data And Implication For Diagenetic Modifications. *Bull. Geol. Soc. Greece* **2010**, *43*, 2553–2561. [CrossRef]
22. Sarkar, B.; Megharaj, M.; Xi, Y.; Naidu, R. Structural characterisation of Arquad® 2HT-75 organobentonites: Surface charge characteristics and environmental application. *J. Hazard. Mater.* **2011**, *195*, 155–161. [CrossRef]
23. Shehab-ElDin, A.N.; Sobh, R.; Rabie, A.; Mohamed, W.; Nasr, H.E. Polyacrylamide Grafted Electrospun Polyamide 6 Nanocomposite Fibers for Drug Delivery Application. *Egypt. J. Chem.* **2022**, *65*, 33–47. [CrossRef]
24. Vaia, R.A.; Teukolsky, R.; Giannelis, E.P. Interlayer Structure and Molecular Environment of Alkylammonium Layered Silicates. *Chem. Mater.* **2022**, *6*, 1017–1022. [CrossRef]
25. Petit, S.; Madejova, J.M. Fourier Transform Infrared Spectroscopy. *Dev. Clay Sci.* **2013**, *5*, 213–231. [CrossRef]
26. Madejová, J. FTIR techniques in clay mineral studies. *Vib. Spectrosc.* **2003**, *31*, 1–10. [CrossRef]
27. Jankovič, L.; Škorňa, P.; Rodriguez, D.; Scholtzová, E. Preparation, characterization and adsorption properties of tetraalkylphosphonium organobeidellites. *Appl. Clay Sci.* **2021**, *204*, 106243. [CrossRef]
28. Hajibeygi, M.; Shabanian, M. The effect of organo-modified silicate nanolayers on the oxygen and water vapor barrier properties of poly(lactic acid). *J. Chin. Chem. Soc.* **2018**, *65*, 1340–1346. [CrossRef]

Disclaimer/Publisher's Note: The statements, opinions and data contained in all publications are solely those of the individual author(s) and contributor(s) and not of MDPI and/or the editor(s). MDPI and/or the editor(s) disclaim responsibility for any injury to people or property resulting from any ideas, methods, instructions or products referred to in the content.